Transactions of JWRI, Vol. 37 (2008), No. 1

Study on Welding Inherent Deformations in Welded Structural Materials†

WANG Rui *, RASHED Sherif **, SERIZAWA Hisashi*, MURAKAWA Hidekazu**** and Jianxun ZHANG *******

Abstract

It is meaningful to predict welding deformation in practical time and to apply these data in welding industry. In this paper, the inherent deformations of beading on plate welding and fillet welding are studied. A 3D thermal-elastic-plastic FEM based on interactive substructure method (ISM) is used to predict the welding deformations. Experiments are carried out to verify the computation results. Based on the computation results, the inverse analysis method is proposed to estimate the inherent deformations. Using inherent deformations, welding deformation can be accurately reproduced by elastic FEM which is much more practical and efficient. Finally, a database of inherent deformations on bead on plate welding and fillet welding including 8 different materials is developed. Meanwhile, the relationship of welding heat input and inherent deformations is discussed. The effectiveness of this method is also confirmed by experimental results.

KEY WORDS: (FEM) (Welding distortion) (Inherent deformation) (Inverse analysis) (Inherent deformation database)

1. Introduction

Welding is widely used in shipbuilding, aerospace and automotive industries for assembling various products. However, welding distortion is one of inevitable problems during welding. Welding distortion has an adverse effect on fabrication precision, structures function, productivity and increase fabrication costs. Therefore, an analysis method to estimate welding distortion avoiding welding distortion problems at industrial production is essential.

Finite element techniques have been used in the prediction of welding residual stress and distortion for more than three decades [1~6]. Some useful simplified formulae and effecting factors for predicting welding distortion have been presented. However, most of them just discuss the specified welding problem. So it is important to create the database about welding distortion for typical welding joints that is useful for predicting the welding distortion in practical welding industry.

Generally, the welding deformations are classified into four fundamental types, transverse shrinkage, longitudinal shrinkage, transverse bending, and longitudinal bending. These four types of deformations can be regarded as fundamental components of the inherent deformations due to welding. Assuming the inherent strain is the initial strain, welding deformation can be easily predicted by elastic finite element analysis, omitting the complicated thermal elastic-plastic finite element analysis. The inherent strain method is more practical and efficient. Ueda et al. [7, 8] studied the characteristic distributions of inherent strains in typical weld joints and employed inherent strains to predict the welding residual stress. Murakawa et al. [9~11] used a simplified analysis model to obtain inherent strain. They represented the inherent strain as a function of the highest temperature and degree of restraint. Based on the inherent strain method, welding deformation and residual stress were investigated. Jang et al. [12, 13] estimated the inherent strain region and investigated the inherent strain as a function of the mechanical melting temperature and the degree of restraint, at the same time welding deformations in large structures were predicted. Liang et al. [14, 15] using an inverse analysis method studied the characteristic distributions of inherent strains in bead on plate welding and used them to predict the welding deformations. Deng et al. [16] using the inherent strain method combined with thermal elastic-plastic finite element analysis predicted the welding distortion in large structures.

In this study, a database of inherent deformations according to 8 different materials and 144 computation cased is created and the welding parametric effects on inherent deformations are also discussed. First three-dimension thermal-elastic-plastic finite element

† Received on July 11, 2008
* Foreign Visiting Researcher, Xi'an Jiaotong University
** Specially Appointed Professor
*** Associate professor
*** * Professor
***** Professor, Xi'an Jiaotong University
Transactions of JWRI is published by Joining and Welding Research Institute, Osaka University, Ibaraki, Osaka 567-0047, Japan

simulation of interactive substructure method (ISM) is used to predict the welding deformations of typical welding joints, bead on plate welding joints and fillet welding joints. Meanwhile, based on the inverse analysis method, the inherent deformations are estimated by thermal-elastic-plastic FEM computation results. Further, using inherent deformations, the elastic FEM is employed as the forward analysis to reproduce the welding distortions. By comparing with the experiment results, the effectiveness of the simulation result is confirmed.

2. Experiment procedure

Experiments are conducted to verify the effectiveness of the numerical results. Two typical welding joints, namely bead on plate welding joint and fillet welding joint are fabricated and their welding temperature and deformations are measured. The welding method used in the experiment is CO2 gas metal arc welding. The base metals are SS400 carbon steel and SUS304 stainless steel. The filler materials are MGS-50 and GFW308L, respectively.

For bead on plate welding, experimental set up is shown in **Fig.1.** The plate sizes are 200mm×200mm. For fillet welding, the size of flange is 200mm×200mm and that of web is 200mm×50mm, and the experimental set up is shown in **Fig.2.** The plate thickness and welding conditions for bead on plate welding and fillet welding are given in **Table 1.**

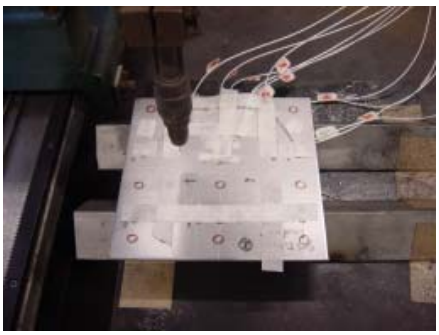

Fig.1. Experiment set up of bead on plate welding

Fig.2. Experiment set up of fillet welding

Table 1 Welding condition.

Case No.	Joint	Material	Plate thickness (mm)	Current (A)	Voltage (V)	Speed (cm/min)	Wire feed rate (mm/s)
1	Bead on plate welding	SS400	3.2	140	24.5	50	53
2	Bead on plate welding	SUS304	5.0	120	28	90	80
3	Fillet welding	SS400(pass 1)	6.0-4.5	180	24	30	69
		SS400(pass 2)	6.0-4.5	175	24	30	69
4	Fillet welding	SUS304(pass 1)	6.0-5.0	140	28.5	35	88
		SUS304(pass 2)	6.0-5.0	135	28.5	35	87

3. Prediction of welding deformation

In general, two methods can be used to obtain the inherent deformations. One is the experimental method and the other is numerical simulation using thermal elastic plastic FEM. In this section, two methods of thermal elastic plastic FEM and elastic FEM are used to estimate the welding distortion, respectively. First, welding deformations are analyzed by three-dimension (3D) thermal elastic plastic FEM using interactive substructure method (ISM) [17]. Meanwhile, the distribution of inherent deformations for bead on plate welding and fillet welding can be computed by inverse analysis method [14]. Then, using inherent deformations as initial deformation, elastic shell FEM can be used to reproduce the welding deformation.

3.1 3-D thermal elastic plastic finite element model

In this investigation, the 3D uncoupled thermal-mechanical analysis is adopted. First, thermal analysis is computed. Then, the temperature history is employed as a thermal load in the subsequent mechanical analysis. Temperature dependent material properties are incorporated in the thermal and mechanical analysis. **Fig.3** shows the finite element mesh models of bead on plate welding and fillet welding which were used in the simulation. For the bead on plate model, the length of the plate is uniformly divided into 50 and 4 elements in the welding and thickness direction. It results in 9046 nodes and 6968 elements. It has a finer mesh grid in the welding zone. For fillet welding model, the mesh method is the same as for bead on plate welding. The FEM model has 18309 nodes and 14400 elements. The dimensions of the finite element model and the boundary conditions (shown in **Fig.3** by arrows on specimens) are the same as those of used in the experimental specimens.

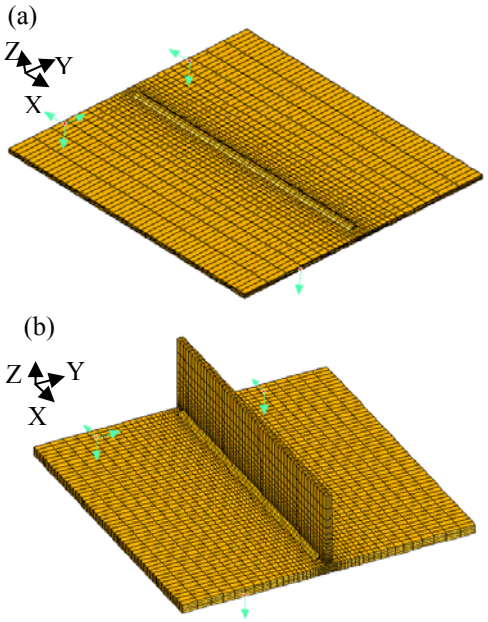

Fig.3. Finite element model: (a) bead on plate welding of case 1, and (b) fillet welding of case 3

3.1.1 Computation results of ISM

Welding temperature and distortions including, transverse shrinkage, angular distortion, and longitudinal shrinkage are predicted for bead on plate welding and fillet welding.

Fig.4 shows the comparison of fusion boundaries between experiment results and computation results from case1 to case 4. The predictions capture the overall dimensions of the fusion boundaries. From these figures it can be concluded that the overall macrosection shapes of computational and experimental results are identical. The comparison results validate the effectiveness of thermal analysis.

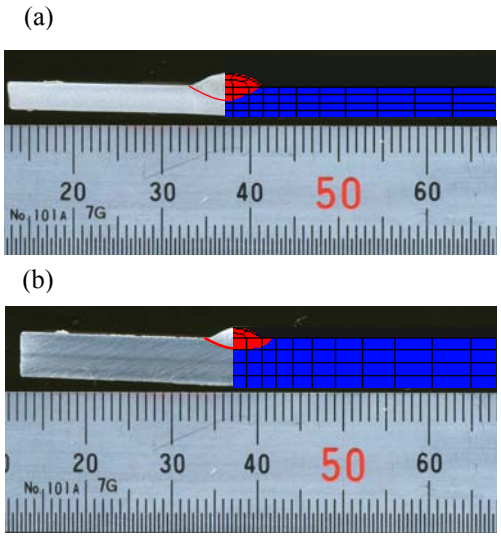

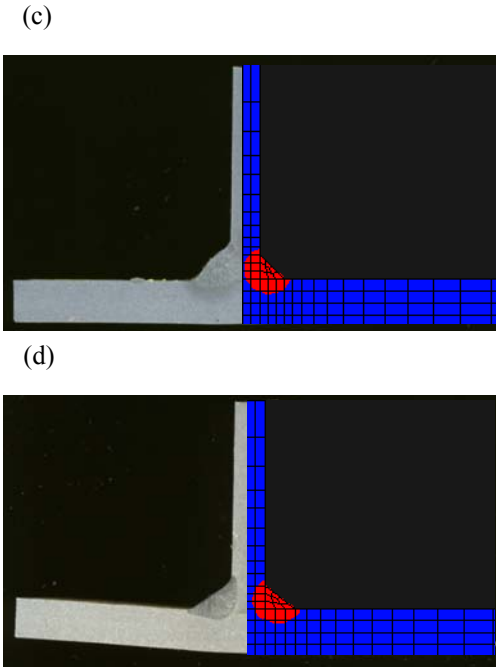

Fig.4. Temperature results: (a) case 1, (b) case 2, (c) case 3, and (d) case 4

Fig.5~ Fig.7 show the comparison results of welding distortion between experiment and computation. Through the comparison of computation with experimental results, it can be observed that the computation results are in excellent agreement with experiment results. The welding distortions can be accurately predicted by ISM. The distortion results show that there are not large differences of welding deformations along the welding direction. Therefore, the deformations can be assumed to distribute uniformly along the weld line.

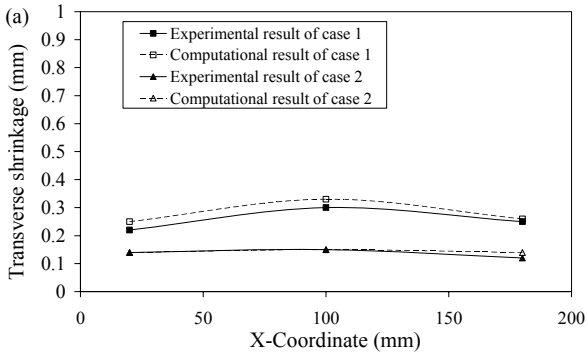

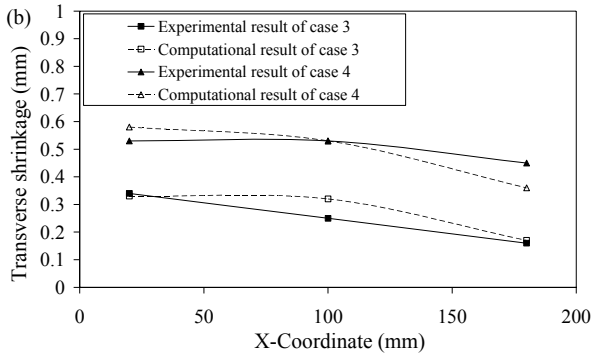

Fig.5. Transverse shrinkage: (a) bead on plate welding, and (b) fillet welding

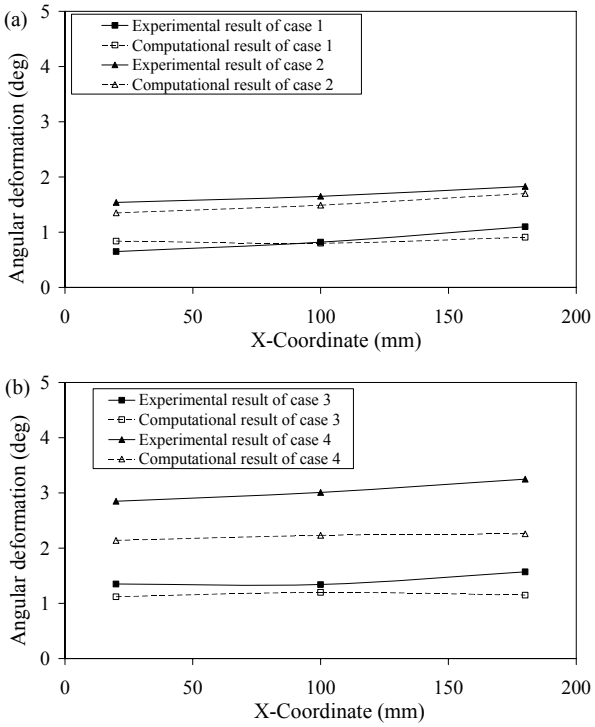

Fig.6. Angular distortion: (a) bead on plate welding, and (b) fillet welding

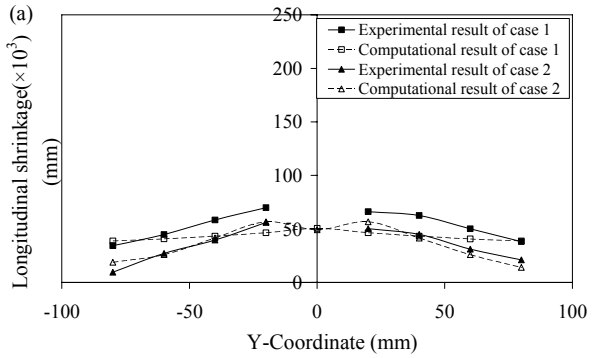

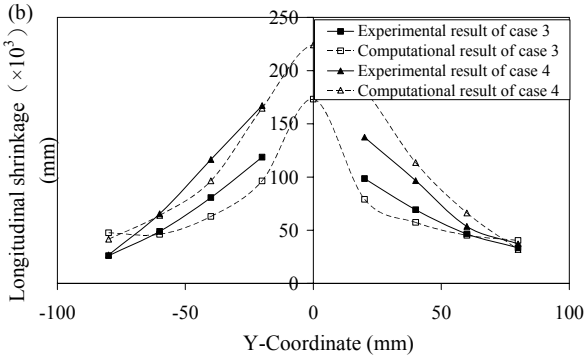

Fig.7. Longitudinal shrinkage: (a) bead on plate welding, (b) fillet welding

3.2 Elastic FEM analysis of welding deformation

The welding deformation is assumed to be caused by four components of inherent deformation, namely longitudinal shrinkage (δ_x^i), transverse shrinkage (δ_y^i), longitudinal bending (θ_x^i), and transverse bending (θ_y^i). These four components are defined by the following equations:

$$\delta_x^i = \int \varepsilon_x^i dydz / h \tag{1}$$

$$\delta_y^i = \int \varepsilon_y^i dydz / h \tag{2}$$

$$\theta_x^i = \int \varepsilon_x^i (z - h/2)/(h^3/12) dydz \tag{3}$$

$$\theta_y^i = \int \varepsilon_y^i (z - h/2)/(h^3/12) dydz \tag{4}$$

Where x is welding direction, y is the direction vertical to welding direction, h is the thickness of plate, ε_x^i is the inherent strain in the X direction, and ε_y^i is the inherent strain in the Y direction.

We use the inherent deformation method, in which the inherent deformations are introduced into the elastic FE analysis, to predict the welding distortion. On the contrary, if the welding deformations are given from experimental measurements or thermal elastic plastic FE analysis, the inherent deformation can be calculated by the method of inverse analysis [14].

In this section, two computation cases, case 2 and case 3 (as shown in table1) are taken as examples to describe the prediction results of welding distortion using inherent deformation method. **Fig.8 (a)** and **(b)** show the shell models of case 2 and case 3, respectively. The areas where the inherent deformations are introduced are shown in large mesh size. The mesh of the shell model is the same as 3-D thermal elastic plastic finite element model.

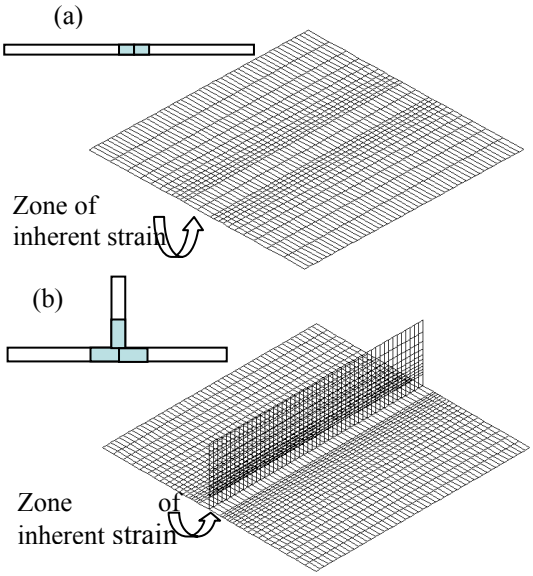

Fig.8. The shell model for elastic analysis: (a) bead on plate welding of case 2, and (b) fillet welding of case 3

3.2.1 Computation results of elastic FEM

As one of the computation results, the angular deformation distributions are shown in **Fig.9.** Meanwhile, the computational results of angular deformation distributions by thermal elastic plastic FE analysis are shown in **Fig.10.** The comparison of deformations accuracy of experiment and those calculated from the elastic FE analysis are compared in **Fig.11.** As seen from **Figs 9-11**, the prediction results of welding deformation by inherent deformation method coincide fairly well with those by thermal elastic plastic FE analysis. These results indicate that inherent deformations method is effective for predicting welding distortion. Using this method, an elastic shell model is used to accurately predict the welding deformations. The computational time by elastic FEM is much shorter than thermal-elastic-plastic FEM.

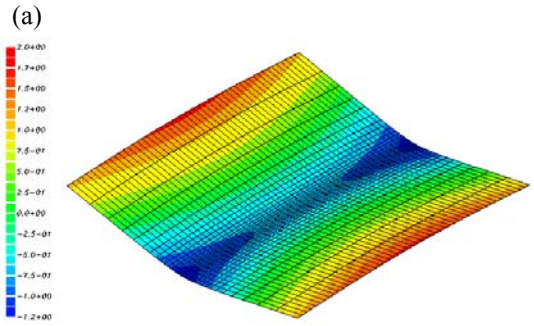

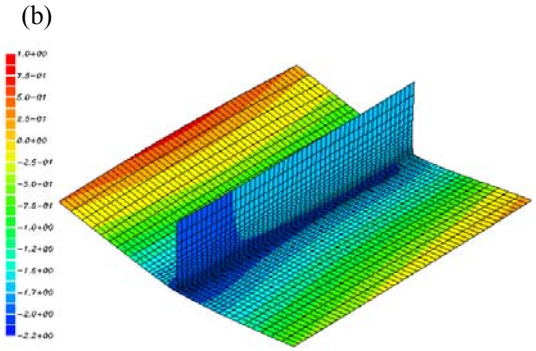

Fig.9 Prediction of welding deformation by elastic FEM: (a) bead on plate welding of case 2, and (b) fillet welding of case 3

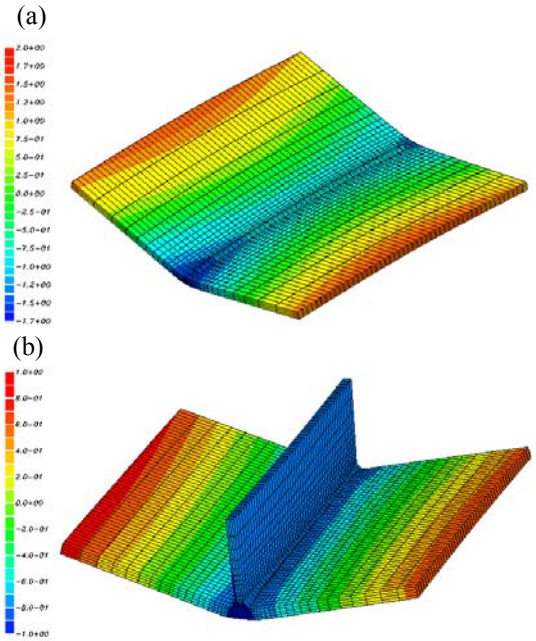

Fig.10. Prediction of welding deformation by elastic-plastic FEM: (a) bead on plate welding of case 2, and (b) fillet welding of case 3

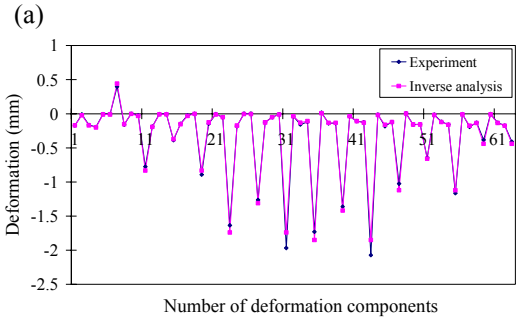

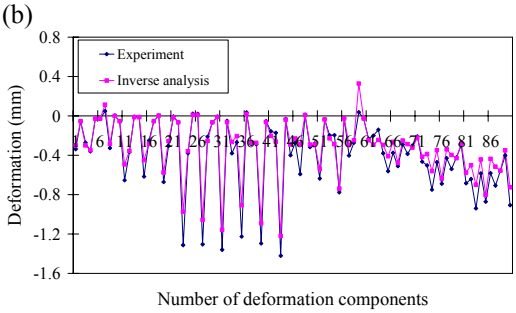

Fig.11. The comparison of deformation measurement and forward analysis: (a) bead on plate welding of case 2, and (b) fillet welding of case 3

4 The database of inherent deformation on different materials

The inherent deformations are mainly determined by the welding heat input, the thickness of members and the type of welding joint [18~20]. Base on the above analysis, the inherent deformations can be accurately estimated by inverse analysis. Once the relation between inherent deformation and welding parameter is created, the welding deformation of welded structure can be predicted by elastic FEM. Thus, the idea of building up a database of inherent deformation is important in predicting welding distortions, especially for large welding structures. Using the results of inherent deformation database, it can easily demonstrate how much deformation will be produced in a given welding heat input condition.

4.1 Computation cases

The database of inherent deformation has been built up for 8 different materials. The range of parameters used in the computation is according to **table 2**.

Table 2 Range of parameters for computation cases

Welding joint	Plate thickness (mm)	Welding current (A)	Welding voltage (V)	Welding speed (mm/s)	Material
Bead on plate joint	3, 3.2, 3.6, 4, 4.5, 5	80-155	23-28	6-15	SUS304, SS400, HT570, HT780, SUS316, SUS430, SPH270D, SPH440D
Fillet joint	4.5, 5, 6, 8	130-185	24-28.5	5-6	

4.2 Computation results of bead on plate welding

The inherent deformations are closely related with welding heat input (Q), the thickness of members (h) and the type of welding joint. In case of bead on plate welding, all of the welding heat input is given to the welding plate as shown in **Fig.12.** The relationship of inherent deformations with bead on plate welding can be defined as the relationship of inherent deformations with parameter $Q_{total/h}^2$.

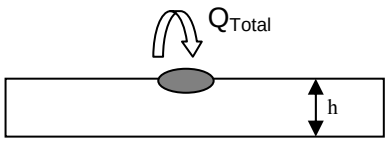

Fig.12. Heat input distribution in bead on plate welding joint

4.2.1 Transverse shrinkage

The relation of transverse shrinkage with welding heat input in bead on plate welding has been studied by [18, 19]. The transverse shrinkage (TS) can be expressed in the following equation:

$$TS/h = \frac{2.85\times10^{-3}Q}{h^2} \quad (5)$$

Where, Q is welding heat input, h is plate thickness.

The variation characteristics of transverse shrinkage with $Q_{total/h}^2$ for bead on plate welding are shown in **Fig.13.** The research results in paper [18] and in this study are shown in **Fig.13 (a)** and **(b)**, respectively. For **Fig.13 (b)**, the different symbols designate different materials and the plots indicate the trend lines. It can be seen from the results that transverse shrinkage (TS/h) linearly increases with $Q_{total/h}^2$. Because of different material properties, the magnitude and tendency of transverse shrinkages show some differences for different materials. The research results in this study show a good agreement with experiment results in paper [18].

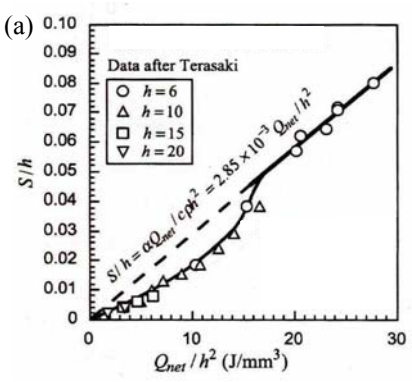

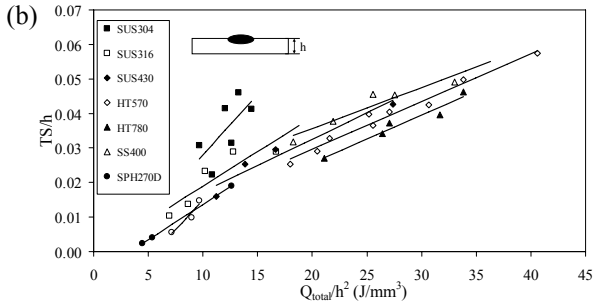

Fig.13. The relation of transverse shrinkage with welding heat input for bead on plate welding: (a) experiment result of transverse shrinkage [18], and (b) computation result of transverse shrinkage

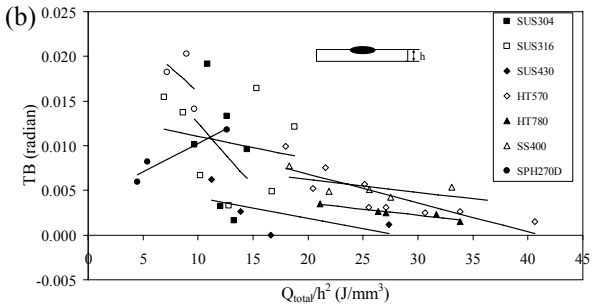

Fig.14. The relation of transverse bending with welding heat input for bead on plate welding: (a) experiment result of transverse bending [18], and (b) computation result of transverse bending

4.2.2 Transverse bending

Transverse bending (TB) on bead on plate welding can be theoretically predicted by the following equation [18]:

$$TB = \frac{0.1061Q^*}{(Q^* - 6.16)^2 + 73.6} \tag{6}$$

Where, Q* is Q/h^2, Q is welding heat input, h is plate thickness.

The variation characteristics of transverse bending with $Q_{total/h}{}^2$ for bead on plate welding are shown in **Fig.14.** The research results in paper [18] and in this study are shown in **Fig.14 (a)** and **(b)**, respectively. From **Fig.14 (b)**, it can be seen that transverse bending (TB) appears a contrary characteristic compared with transverse shrinkage when $Q_{total/h}{}^2$ is during 10~30 (J/mm^3). The transverse bending decreases with $Q_{total/h}{}^2$ increasing. The maximum transverse bending (TB) obtained when $Q_{total/h}{}^2$ kept at almost 10 (J/mm^3). Comparing with **Fig.14 (a)**, when welding heat input is smaller than 10 (J/mm^3), the transverse bending is increasing with $Q_{total/h}{}^2$. The transverse bending is decreasing with $Q_{total/h}{}^2$ when $Q_{total/h}{}^2$ is larger than 10 (J/mm^3). The expected research results in this study coincide with experiment results in paper [18].

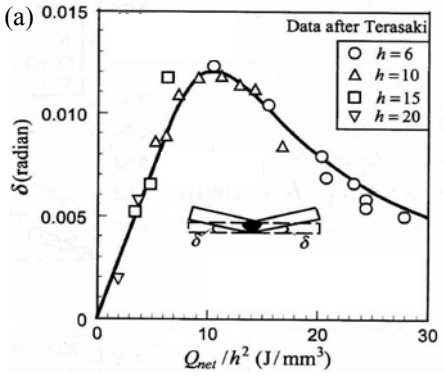

4.2.3 Longitudinal shrinkage

For longitudinal shrinkage, first Tendon Force (F) is calculated by the following formula (Refs 20, 21, 22):

$$F = 0.2Q \tag{7}$$

Where, Q is welding heat input.

Then the Tendon Force (F) is converted to equivalent longitudinal shrinkage (LS) expressed by the following equation:

$$F = EhLS \tag{8}$$

Where, E is Young's Modulus, h is plate thickness.

For a given welding heat input, according to equations (7) and (8), the approximate expression for LS can be described as:

$$LS/h = \frac{0.2}{E}\left(\frac{Q}{h^2}\right) \tag{9}$$

Fig.15 shows the research results of longitudinal shrinkage in this study. As seen from the figure, the longitudinal shrinkage (LS/h) linearly increases with $Q_{total/h}{}^2$. The research results coincide with the theoretical prediction equation. The magnitude of longitudinal shrinkage is much smaller than transverse shrinkage when $Q_{total/h}{}^2$ changes from 10 (J/mm^3) to 40 (J/mm^3).

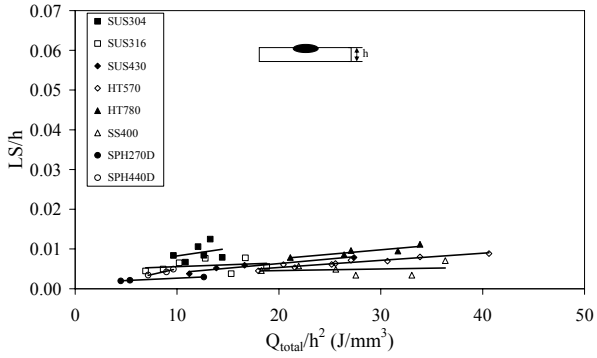

Fig.15. The relation of longitudinal shrinkage with welding heat input in bead on plate welding

4.2.4 Longitudinal bending

Fig.16 shows the research results of longitudinal bending. From the figure, it is seen that the longitudinal bending (LB) decreases a little with $Q_{total/h}{}^2$ increasing. Because of different material properties, the changing extent of longitudinal bending shows a little difference. However, the magnitude of longitudinal bending is much smaller than transverse bending for all cases.

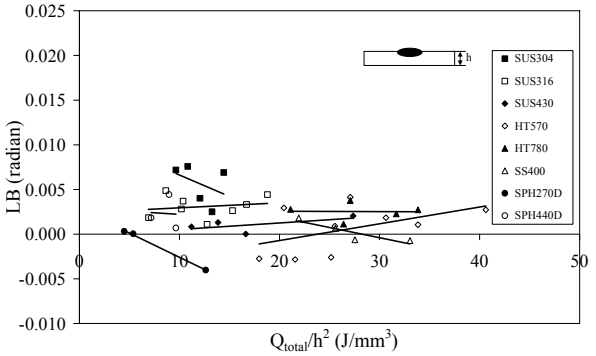

Fig.16. The relation of longitudinal bending with welding heat input in bead on plate welding

4.3 Computation results of fillet welding

In the case of fillet welding, as shown in **Fig.17**, the welding heat input is given to both the flange and web. The distribution of heat input in the flange and the web are defined by the following equations [15]:

$$Q_{web} = \frac{h_w}{2h_f + h_w} Q_{total} = \frac{h_w}{2h_f + h_w}(Q_L + Q_R) \tag{10}$$

$$Q_{flange} = \frac{2h_f}{2h_f + h_w} Q_{total} = \frac{2h_f}{2h_f + h_w}(Q_L + Q_R) \tag{11}$$

Where, Q_{total} is total heat input, QL and QR are heat input in left side and right side, respectively, h_w and h_f are the thickness of web and flange, respectively.

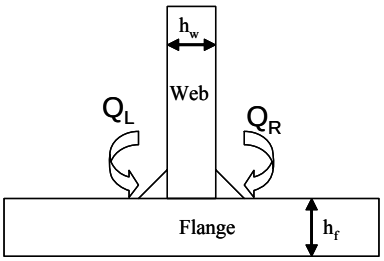

Fig.17. Heat input distribution in fillet welding joint

According to equation (10) and (11), the heat input for the flange and the web of fillet welding are different. So the fillet welding joint will be divided into the flange and the web for discussion, respectively. The relationship of welding inherent deformation with fillet welding can also be defined as the relationship of welding inherent deformation with Q/h^2.

4.3.1 Transverse shrinkage

The relation of transverse shrinkage (TS) with Q/h^2 on flange and web of fillet welding is shown in **Fig.18 (a)** and **(b)**. It is seen from the results that transverse shrinkage (TS) both on flange and web linearly increase with Q/h^2. Comparing between **Fig.18 (a)** and **Fig.18 (b)**, the transverse shrinkage (TS) of the flange is larger than that of the web.

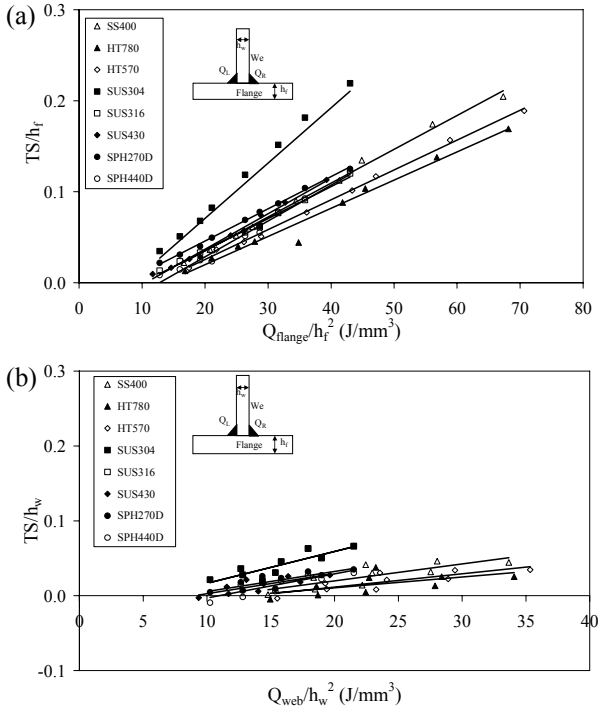

Fig.18. The relation of transverse shrinkage with welding heat input in fillet welding: (a) transverse shrinkage on flange, and (b) transverse shrinkage on web

4.3.2 Transverse bending

Fig.19 (a) and **(b)** show the relationship of transverse bending (TB) of flange and web with Q/h^2 on fillet welding. From **Fig.19**, it is seen that transverse bending linearly increases with Q/h^2 increasing when Q/h^2 is larger than 10 (J/mm^3). Comparing between **Fig.19 (a)** and **Fig.19 (b)** shows that transverse bending in the web changes slowly with Q/h^2 increasing. The magnitudes of transverse bending in the web almost keep constant with Q/h^2 increasing. It can be concluded that Q/h^2 has less influence on transverse bending in the web of fillet welding.

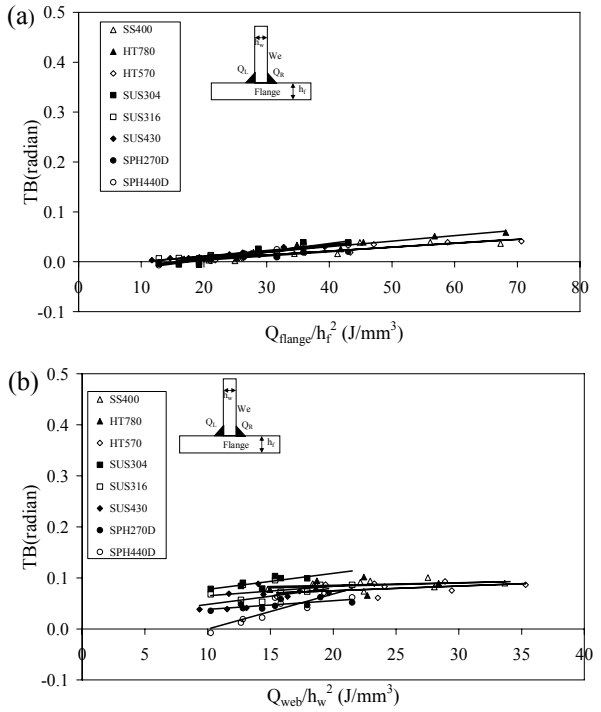

Fig.19. The relation of transverse bending with welding heat input in fillet welding: (a) transverse bending on flange, and (b) transverse bending on web

4.3.3 Longitudinal shrinkage

The theoretical calculation of longitudinal shrinkage for fillet welding is the same as for bead on plate welding. The longitudinal shrinkage can be calculated from the Tendon Force[21]. In this study, the relation of longitudinal shrinkage (LS) with Q/h^2 in fillet welding is shown in **Fig.20.** From **Fig.20 (a)** and **(b)**, it is seen that longitudinal shrinkage linearly increases with Q/h^2. Comparing between **Fig.20 (a)** and **(b)**, it can be seen that the magnitudes of longitudinal shrinkage in the flange are a little larger than those in the web.

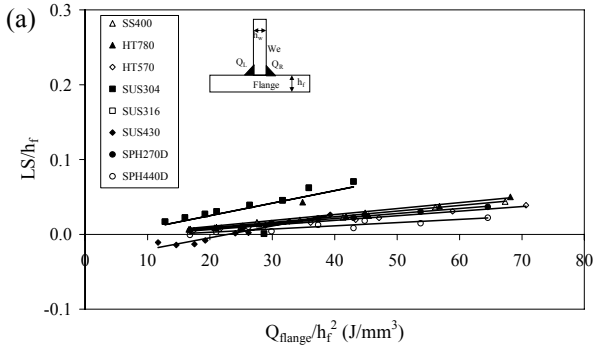

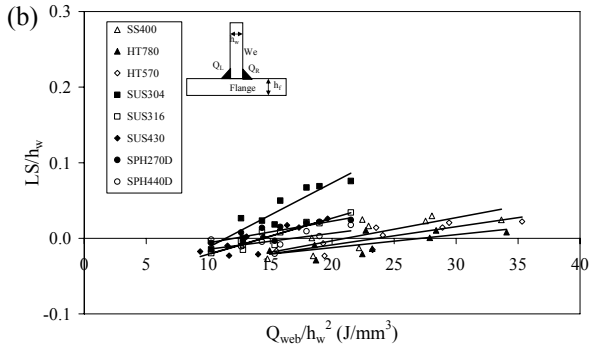

Fig.20. The relation of longitudinal shrinkage with welding heat input in fillet welding: (a) longitudinal shrinkage on flange, and (b) longitudinal shrinkage on web

4.3.4 Longitudinal bending

The relation of longitudinal bending (LB) of flange and web with Q/h^2 in fillet welding is shown in **Fig.21 (a)** and **(b)**. From **Fig.21**, it is seen that longitudinal bending linearly increases with Q/h^2 when Q/h^2 is larger than 10 (J/mm^3). Comparing the computation results between **Fig.21 (a)** and **Fig.21 (b)** show that longitudinal bending in the web changes slowly with the Q/h^2 increasing.

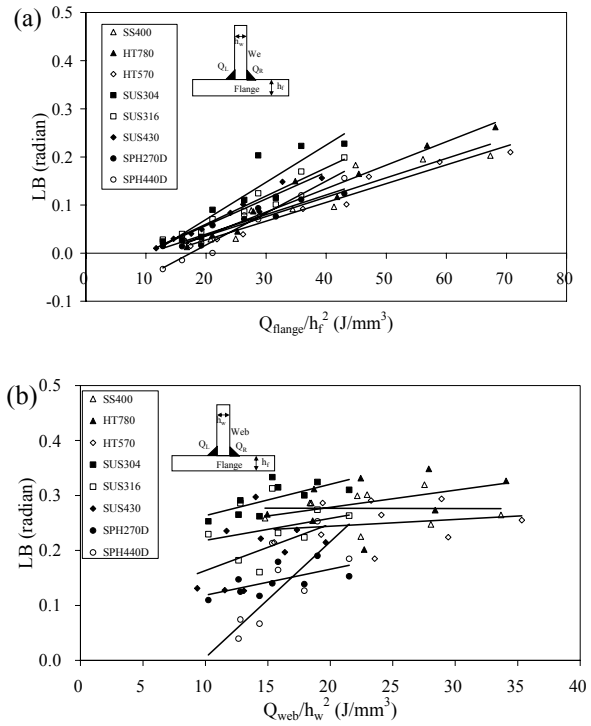

Fig.21. The relation of longitudinal bending with welding heat input in fillet welding: (a) longitudinal bending on flange, and (b) longitudinal bending on web

6 Conclusions

According to the research results in the present work, the conclusions are summarized as following:

(1) Using ISM, the welding deformation can be numerically predicted in typical welding joints. The

prediction results are in good agreement with experiment results.

(2) Inherent deformations can be estimated by inverse analysis. Furthermore, welding deformation can be estimated by elastic FEM based on inherent deformations results. The complicated thermal elastic plastic problem is translated into a simple elastic problem. The elastic FEM can save much computation time. The comparison between computation and experiment results concludes that the elastic FEM result is validated.

(3) The approach and model used in this study are shown to be effective and efficient to estimate the inherent deformations of typical welding joints. A database of inherent deformations based on 8 different materials is developed based on the computation results in this study.

(4) The effect of Q/h^2 for inherent deformations on bead on plate welding is investigated. The analysis results show that for bead on plate welding, the transverse shrinkage is linearly increasing with Q/h^2. The transverse bending is decreasing with Q/h^2 when Q/h^2 changes from 10 to 40 (J/mm^3). The maximum transverse bending obtained when the Q/h^2 is kept at 10 (J/mm^3). The longitudinal shrinkage is linearly increasing with Q/h^2. The magnitude of longitudinal shrinkage is much smaller than transverse shrinkage. The longitudinal bending decreases a little with Q/h^2 increasing. The magnitude of longitudinal bending is smaller than transverse bending.

(5) The effect of Q/h^2 on inherent deformations of fillet welding is also investigated in this study. The research results indicate that when heat input changes from 10 to 40 (J/mm^3), the inherent deformations linearly increase with the increasing of Q/h^2 on fillet welding. Comparing the computation results of inherent deformations between the flange and the web of fillet welding, the results show that the magnitudes of inherent deformations on the web change little with Q/h^2 increasing. The Q/h^2 has less effect on the inherent deformations in the web of fillet welding when Q/h^2 changes from 10 to 40 (J/mm^3).

Acknowledgements

This research was the results of "Survey and research on building welding inherent deformation database and data generation", which was supported by the New Energy and Industrial Technology Development Organization (NEDO).

References

1) V. J. Papazoglou and K.Masubuchi. Weld. J. 57(9): 251−262, 1978.
2) W. Woo, H. Choo, D. W. Brown, Z. Feng, P. K. Liaw. Mater. Sci. Eng. A. 437: 64-69, 2006.
3) C.L.Tsai, S.C.Park, W.T.Cheng. Weld. J. 78(5):157-165, 1999.
4) A.K.Dhingra, C.L.Murphy. Sci. Technol. Weld. Join. 10(5): 528-536, 2005.
5) M. A. Zaeem, M.R.Nami, M.H.Kadivar. Sci. Forum. 519-521:1187-1192, 2006.
6) P.Dong. Sci. Technol. Weld. Join. 10(4):389-398, 2005.
7) Y. Ueda, M.G.Yuan. J. Engrg. Mater. Technol. 115 (10): 417-423, 1993.
8) M.G.Yuan, Y.Ueda. J. Engrg. Mater. Technol. 118 (4):229-234, 1996.
9) H. Murakawa, Y.Luo, Y. Ueda. J. Soc. Naval Architect. Jpn. 180: 739-751, 1996.
10) Y.Luo, H. Murakawa, Y. Ueda. J. Soc. Naval Architect. Jpn. 182: 783-793, 1997.
11) Y.Luo, H. Murakawa, Y. Ueda. J. Soc. Naval Architect. Jpn., 183: 323-333, 1997.
12) C.D.Jang, C.H.Lee, D.E.Ko. Proc. Instn. Mech. Engrs. 216: 133-143, 2002.
13) S.I.Seo, C.D.Jang. J.Ship Prod. 15(2): 73-81, 1999.
14) W. Liang, S.J. Sone, M. Tejima, H. Serizawa, H.Murakawa. Transactions of JWRI. 33(1): 45-51, 2004.
15) W.Liang, D.A. Deng, H.Murakawa. Transactions of JWRI. 34(1): 113-123, 2005.
16) D. A. Deng, H. Murakawa, W. Liang. Comput. Methods Appl. Mech. Engrg. 196: 4613-4627, 2007.
17) H.Nishikawa, H.Serizawa, H.Murakawa. Sci. Technol. Weld. Join. 12(2): 147-152, 2007.
18) K. Satoh, T. Terasaki. Quar. J. JWS. 45(4): 302-308, 1976.
19) Y.Takeda. J. Ship Prod. 18(2): 99-104, 2002.
20) T.Terasaki, T.Ishimura, K.Matsuishi, T.Akiyama. Quar. J. JWS. 20(1): 136-142, 2002.
21) T.Terasaki, T.Kitamura, I. Kidota, T.Ishimura, S.Hamashima. Quar. J. JWS. 21(1): 81-86, 2003.
22) C.L.M.Cottrell. Weld. J. 32: 257-272, 1953.